Structure of the Signal Sequences for Two Mitochondrial Matrix Proteins That Are Not Proteolytically Processed upon Import†

Philip K. Hammen,‡ David G. Gorenstein,§ and Henry Weiner*,‡

Departments of Biochemistry and Chemistry, Purdue University, West Lafayette, Indiana 47907

Received February 23, 1994; Revised Manuscript Received May 10, 1994®

ABSTRACT: The N-terminal sequences of rhodanese and 3-oxoacyl-CoA thiolase, two mitochondrial matrix proteins that are not proteolytically processed upon import, have been studied by NMR and CD spectroscopy. In aqueous trifluoroethanol, in the presence of micelles, and in the presence of small unilamellar vesicles (SUVs), these peptides form α-helical structures beginning near the N-terminus and extending, continuously, for at least three helical turns. This result is consistent with a previous finding that a mutant rat liver mitochondrial aldehyde dehydrogenase signal sequence we designed, which formed a continuous α-helix, could successfully direct protein import but was not proteolytically processed (Thornton, K., Wang, Y., Weiner, H., & Gorenstein, D. G. (1993) *J. Biol. Chem. 268*, 19906–19914). From these three examples, a model is developed which suggests that a mitochondrial signal sequence that has an N-terminal α-helix longer than 11 residues can take on the necessary conformation to be imported but cannot adopt the necessary conformation to be processed.

The import of nuclear encoded proteins into mitochondria is a complex process that appears to involve several steps. These include recognition of the precursor protein at the mitochondrial surface, subsequent recognition by import machinery located in the membrane, transport across the membrane, and ultimate sorting into the correct mitochondrial compartment (which may involve transport back through the inner mitochondrial membrane). For most proteins, the signal sequence is removed after import by a proteolytic enzyme (Géli 1993; Arretz *et al.*, 1994). All the information necessary for successful mitochondrial import and subsequent proteolytic processing is located in the signal sequence, which occurs at the N-terminus of the precursor protein (Hannavy *et al.*, 1993; Hartl *et al.*, 1989; Horwich *et al.*, 1991).

Following import, the signal sequences of a few proteins are not removed by the protease. Two mammalian mitochondrial matrix proteins which are not processed are rhodanese and 3-oxoacyl-CoA thiolase. Bovine rhodanese is a protein of known primary and tertiary structure (Ploegman *et al.*, 1978). In the crystal structure, residues 11–22 form an α-helix. Studies involving synthetic peptides corresponding to the N-terminus of the mature protein have demonstrated α-helix-forming propensity when in contact with liposomes made of cardiolipin, but not phosphatidylcholine (Zardeneta *et al.*, 1992). The tertiary structure of 3-oxoacyl-CoA thiolase is not known. However, the primary structure of the rat enzyme is known from cDNA analysis (Arakawa *et al.*, 1987). The first 14–16 residues of 3-oxoacyl-CoA thiolase have been shown to be sufficient to direct the import of a "passenger protein" into mitochondria (Arakawa *et al.*, 1990).

The reasons why certain proteins are not proteolytically processed after import are not clear. There is no specific amino acid identity or sequence identity that can be associated with proteolysis. It has been suggested on the basis of statistical analyses (Hartl *et al.*, 1989; Gavel & von Heijne, 1990) that a basic residue, particularly R, is located two residues to the N-terminal side of the cleavage site in about half of the sequences, along with some less populous motifs. Proteolytic processing of the ornithine transcarbamylase signal sequence is achieved in two steps, first after N24, then after Q32. Replacement of R23 in the ornithine transcarbamylase signal sequence by K, N, and A led to a partial decrease in processing, but replacement by glycine caused processing to be abolished (Horwich *et al.*, 1987). This correlation with helix-forming propensity has been used to suggest that the signal protease recognizes a secondary structure, perhaps in conjunction with a basic amino acid (Horwich *et al.*, 1991). Since the signal sequences are already thought to form amphiphilic secondary structures (von Heijne 1986; Roise *et al.*, 1987), this would be a convenient structure for recognition by the protease. An alternative explanation has been proposed (Jeng & Weiner, 1991; Zardeneta *et al.*, 1992) that suggests that the signal sequence interacts strongly with the inner mitochondrial membrane. This membrane contains an unusually large amount of the negatively charged phospholipid cardiolipin. It has been shown that mitochondrial signal peptides bind tightly to the mitochondrial inner membrane (Pak & Weiner, 1990; Glaser & Cumsky, 1990). It is possible that the positively charged, amphiphilic N-terminus binds tightly to the membrane and is then protected from proteolysis.

To better understand how the signal sequences determine whether processing occurs, knowledge of the signal sequence structure in a structure-promoting environment is essential. A comparison of the structural preferences of signal peptides from nonprocessed proteins with those from processed proteins could provide insight into how the signal sequence structure is involved in proteolytic processing.

The structure of several synthetic mitochondrial signal sequences in lipid-like media has been determined using NMR[1] spectroscopy. The presequence of cytochrome oxidase subunit IV was shown to form an α-helix between residues 3 and 11 in the presence of dodecylphosphatidylcholine micelles (Endo *et al.*, 1989). In the same medium, the synthetic presequence

† Supported by NIH Grant AA05812-11 (H.W.) and by NIH Grant AI27713 (D.G.G). P.K.H. was supported by NIH Training Grant 5T32DK07532-08. H.W. is a recipient of Senior Scientist Award AA00038 from the National Institutes on Alcohol Abuse and Alcoholism. This is Journal Paper 14197 from the Purdue University Agriculture Experiment Station.

* Author to whom correspondence should be addressed.

‡ Department of Biochemistry.

§ Department of Chemistry.

® Abstract published in *Advance ACS Abstracts,* June 15, 1994.

0006-2960/94/0433-8610$04.50/0

Table 1: Synthetic Peptides Corresponding to N-Terminal Sequences of Two Mitochondrial Matrix Proteins That Are Not Processed upon Import

RHODANESE [1-23]	M-V-H-Q-V-L-Y-R-A-L-V-S-T-K-W-L-A-E-S-I-R-S-G
THIOLASE [1-21]	M-A-L-L-R-G-V-F-I-V-A-A-K-R-T-P-F-G-A-Y-G

of rat liver aldehyde dehydrogenase was shown to form an α-helix from residues 2–10 and 14–19 (Karslake *et al.*, 1990). The synthetic presequence of human mitochondrial F_1-ATPase β was shown to form an α-helix from residues 4–10 in 50% TFE solution at 25 °C and from residues 4–10 and 13–20 at 5 °C (Bruch & Hoyt, 1992). Assuming that the structure of the synthetic peptide corresponds to the structure at the N-terminus of the precursor protein, the α-helix nearest to the N-terminus in these proteins consists of less than three turns. These examples form a small, but important, data base of signal sequence structure in proteins that are processed.

In the presequence of rat liver ALDH, residues 11–13, between the two helical regions, have the sequence R-G-P. When this flexible three residue "linker" was removed, the protein was imported into mitochondria, but was not proteolytically processed (Thornton *et al.*, 1993). The synthetic peptide corresponding to this sequence was shown to form an α-helix from R5 to its C-terminus. The helix continued for several residues beyond the normal proteolytic cleavage site into residues that correspond to those in the mature protein. The length of the α-helix nearest to the N-terminus, in this case, was more than three turns.

In the present study, the structures of the N-terminal sequence of rat rhodanese and rat 3-oxoacyl-CoA thiolase have been investigated. The amino acid sequence of each peptide is shown in Table 1. The principle aim was to determine if a correlation exists between the lack of proteolytic processing upon mitochondrial import and the length of the α-helix that the polypeptide sequence tends to form. In addition, the structures obtained add to the limited data base of detailed structural information on mitochondrial signal sequences.

EXPERIMENTAL PROCEDURE

Peptide Synthesis and Purification. Peptides were synthesized in the Macromolecular Structure Laboratory of the Purdue University Biochemistry Department using a 430A ABI solid-state peptide synthesizer. They were purified using a semipreperative Vydac C_{18} reverse-phase (20 cm × 1 cm diameter) HPLC column. Peptide elution was achieved by the application of an acetonitrile gradient. Peptide authenticity was identified by mass spectrometry (rhodanese[1–23] M_r = 2646; thiolase[1–21] M_r = 2239) and verified by amino acid analysis. Peptide concentrations in aqueous buffer were determined from quantitative amino acid analysis.

Liposomes. Liposomes were prepared by mixing the appropriate quantities of egg L-α-lecithin (20 mg/mL in $CHCl_3$; Avanti Polar Lipids) and cardiolipin (4.8 mg/mL in methanol; Sigma) in a clean test tube. Solvent was evaporated with vortexing under a stream of nitrogen gas. The residue was lyophilized for at least 12 h. The headspace air was purged with N_2 and the lipids were resuspended in 50 mM phosphate buffer, pH 5.2, with vortexing. Liposomes were formed by using high-energy ultrasonic irradiation of the lipid suspension for 10–20 min at room temperature (Huang, 1969). Liposome formation was complete when the opaque suspension became clear.

Fluorescence Anisotropy. A SLM 8000 fluorescence spectrophotometer was used for the fluorescence anisotropy measurements. Excitation and emission polarizers were rotated manually to measure the intensity of four fluorescence components, I_{VV}, I_{VH}, I_{HV}, and I_{HH}. Subscripts refer to the orientation of the excitation polarizer (former) and the polarizer used to sample emission (latter) with respect to their vertical or horizontal orientation. The anisotropy was obtained from eq 1, in which the fluorescence intensities that depend

$$I = \frac{I_{VV} - I_{VH}(I_{HV}/I_{HH})}{I_{VV} + 2I_{VH}(I_{HV}/I_{HH})} \quad (1)$$

on the excitation polarizer orientation are used to correct for instrumental dependence on polarization of the emitted beam (Lakowicz, 1983).

Peptide was added to a solution that was 150 μM in lipid in a volume of 2 mL. Several measurements were made for each peptide. For rhodanese[1–23] the final peptide concentration was 0.3 μM. For thiolase[1–21] the final peptide concentration was 8 μM. Fluorescence intensities, obtained after the addition of an equivalent volume of buffer alone, were subtracted from the peptide measurements. Where necessary, fluorescence intensities were corrected for dilution effects. Light scattering from solution turbidity did not interfere with measurements at the concentrations used. All measurements were made at 25.5 °C. Anisotropy values are the averages of the measured values.

Circular Dichroism. Circular dichroism spectra between 250 and 190 nm were obtained on a Jasco J-600 spectropolarimeter at 25 °C. The path length for the samples was 0.1 cm. Baseline spectra for each solvent was obtained prior to the peptide spectra. Peptide concentrations in these measurements ranged from 10–50 μM, without causing significant differences in ellipticities. The secondary structure analyses were carried out using a curve-fitting deconvolution based on standard spectra (Yang *et al.*, 1986).

Nuclear Magnetic Resonance. All nuclear magnetic resonance spectra were obtained on a Varian VXR-500 spectrometer with a basic frequency of 500 MHz. Peptides were dissolved in mixtures of trifluoroethanol and 50 mM phosphate buffer, pH 5.2, to a final concentration of ca. 2 mM. In the case of PC micelles, a solution of perdeuteriododecylphosphatidylcholine (MSD Isotopes) in 50 mM phosphate, pH 5.2, was added to a solution of thiolase[1–21] in 50 mM phosphate, pH 5.2, to bring the final concentrations to 1 mM peptide and 200 mM phosopholipid. All chemical shifts were referenced to an internal standard of sodium perdeutero-3-(trimethylsilyl)-1-propanesulfonate (DSS). The temperature for all NMR spectra was 20 °C.

Two-dimensional spectra were obtained with spectral width of 6000 Hz in both f_1 and f_2 in 2K complex data sets. A total of 300 t_1 increments were obtained using the hypercomplex method to achieve quadrature detection in the second dimension (States *et al.*, 1982). The exception was the NOESY spectrum of rhodanese[1–23], which utilized time-

[1] Abbreviations: NMR, nuclear magnetic resonance; NOESY, two-dimensional nuclear Overhauser effect spectroscopy; TOCSY, two-dimensional total coherence spectroscopy; DQF-COSY, two-dimensional double quantum-filtered coherence spectroscopy; SUV, small unilamellar vesicles; CD, circular dichroism; PC, phosphatidylcholine, SDS, sodium dodecyl sulfate; TFE, trifluoroethanol; ALDH, aldehyde dehydrogenase; COX-IV, cytochrome *c* oxidase subunit IV.

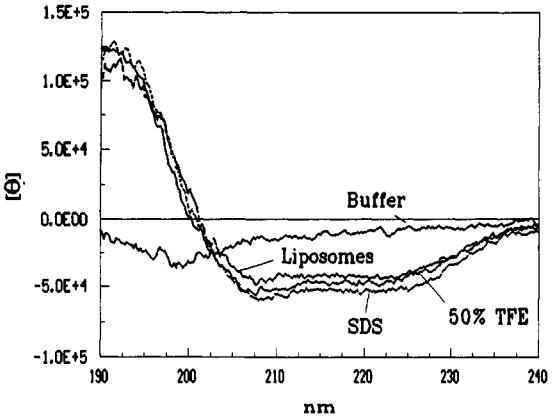

FIGURE 1: Circular dichroism spectra of rhodanese[1–23] in phosphate buffer, in 50% TFE, with SDS micelles, and with SUVs containing 30% cardiolipin/70% egg L-α-lecithin. All solutions were at pH 5.2 and 25 °C.

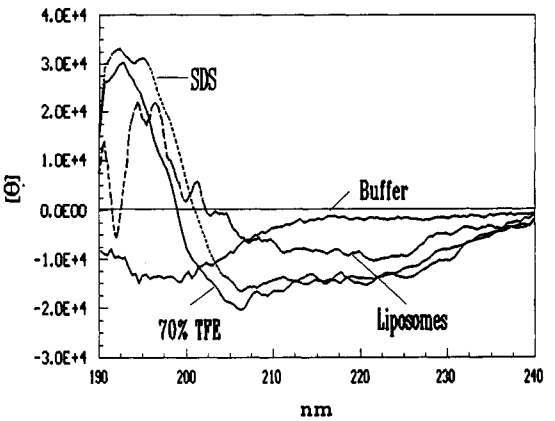

FIGURE 2: Circular dichroism spectra of thiolase[1–21] in 70% TFE, with SDS micelles, and with SUVs containing 30% cardiolipin/70% egg L-α-lecithin. All solutions were at pH 5.2 and 25 °C.

proportioned phase incrementation (TPPI) (Marion & Wüthrich, 1983) to achieve quadrature detection in the second dimension. Fourier transformation was weighted with a 60° shifted sine-bell function. For NOESY experiments, mixing times of 150 ms (rhodanese[1–23]) and 200 ms (thiolase-[1–21]) were used for TFE solutions and 100 ms was used in the presence of micelles.

The TOCSY experiments (Bax & Davis, 1985; Braunschweiler & Ernst, 1983) were performed using a 70 ms MLEV-16 sequence to achieve coherence transfer. DQF-COSY experiments (Piantini *et al.*, 1982; Rance *et al.*, 1983) were performed to help with specific resonance assignments. Data sets were processed on SUN 4 workstations using VNMR software provided by Varian.

RESULTS

Circular Dichroism Spectra of Rhodanese[1–23]. The CD spectrum of rhodanese[1–23] in aqueous buffer, pH 5.2, is that of a polypeptide without defined secondary structure. As increasing amounts of TFE or SDS micelles were added, the CD spectrum changed, indicating the formation of a significant extent of α-helical conformation. In Figure 1, the CD spectra of rhodanese[1–23] in phosphate buffer, in 50% TFE solution, with an approximately 1000-fold excess of SDS micelles, and with excess SUVs containing 30% cardiolipin/70% egg L-α-lecithin are shown. With the exception of the spectrum in buffer, they are essentially identical. When the contributions of secondary structure elements were estimated using spectral deconvolution, the result in each case was 95–99% α-helix. This value is probably an overestimate due to the very intense absorbance between 208 and 225 nm. The present result is consistent with that reported previously for the peptide from the bovine protein (Zardeneta *et al.*, 1992). At the concentrations used for CD and fluorescence measurements (1–100 μM), no apparent aggregation of peptides occurred (data not shown).

Circular Dichroism Spectra of Thiolase[1–21]. The CD spectrum of thiolase[1–21] in aqueous phosphate buffer, pH 5.2, showed no evidence of defined secondary structure. As increasing amounts of TFE or SDS micelles were added, the character of the spectra changed in a way that indicated that the conformation contained some ordered secondary structure. Figure 2, shows the CD spectra of thiolase[1–21] in phosphate buffer, in 70% TFE, with an approximately 1000-fold excess of SDS micelles, and with excess SUVs containing 30% cardiolipin/70% egg L-α-lecithin. When the helical content of the peptide was estimated from the spectra in Figure 2, using spectral deconvolution, some variation was found. In 70% TFE solution, the percentage was 36% α-helix, while in the presence of SDS micelles, the estimated percentage was 44%. α-Helical content was estimated from the molar ellipticity at 222 nm, using the $[\theta]_{222}$ value of −26 500 deg cm^2/dm determined for a 13-residue ribonuclease C peptide (Shoemaker *et al.*, 1987) to represent 100% helix. The calculation for both 70% TFE and micellar solution gives ca. 52% α-helix. The CD spectrum with SUVs containing cardiolipin could not be used to reliably calculate secondary structure by curve-fitting because of the noise between 190 and 200 nm. The noise was probably caused by the formation of colloidal lipid particulates in the sample. However, the position of the ellipticity sign change at 203 nm and the intensity at 222 nm suggest that the amount of helix is less in the presence of SUVs than in 70% TFE or with micelles. Estimation of α-helical content in the presence of SUVs, based on the molar ellipticity at 222 nm, gives ca. 38% helix.

Solution Structure of Rhodanese[1–23] Characterized by NMR. Since CD spectra were nearly identical for 50% TFE solution, SDS micelles, and liposomes, the 50% TFE solution was selected for use in NMR studies. Chemical shift assignments for each amino acid spin system were obtained from analyses of DQF-COSY and TOCSY spectra. All protons with the exception of the Q4 ϵNH protons and the side-chain of L6 were made without the use of NOESY spectra. Sequential residue assignments were made using the NOESY spectrum and the known amino acid sequence (Figure 3). The chemical shift assignments appear in Table 2.

Secondary structure features were assessed by plotting the chemical shift of α-protons relative to the random coil values found in the literature (Wishart *et al.*, 1991). The strong preference toward an upfield shift in residues 4–21 is indicative of an α-helical structure spanning these residues (Figure 4A).

Analyses of inter-residue interactions in the NOESY spectra also indicate that rhodanese[1–23] forms an α-helical structure between residues 4 and 21 in 50% TFE solution (Figure 5). Resolved $H\alpha_i$-HN_{i+3} interactions were observed for Q4-Y7, V5-R8, L6-A9, Y7-L10, V11-K14, S12-W15, A17-I20, and E18-R21. Resolved $H\alpha_i$-$H\beta_{i+3}$ interactions were observed for Q4-Y7, L10-T13, and W15-E18. A resolved $H\alpha_i$-$H\beta_{i+4}$ interaction was observed between V11 and W15. Medium-range interactions that could not definitively assigned, due to spectral overlap, are noted in Figure 5. The observed interactions are characteristic of an α-helical conformation extending from Q4 to R21.

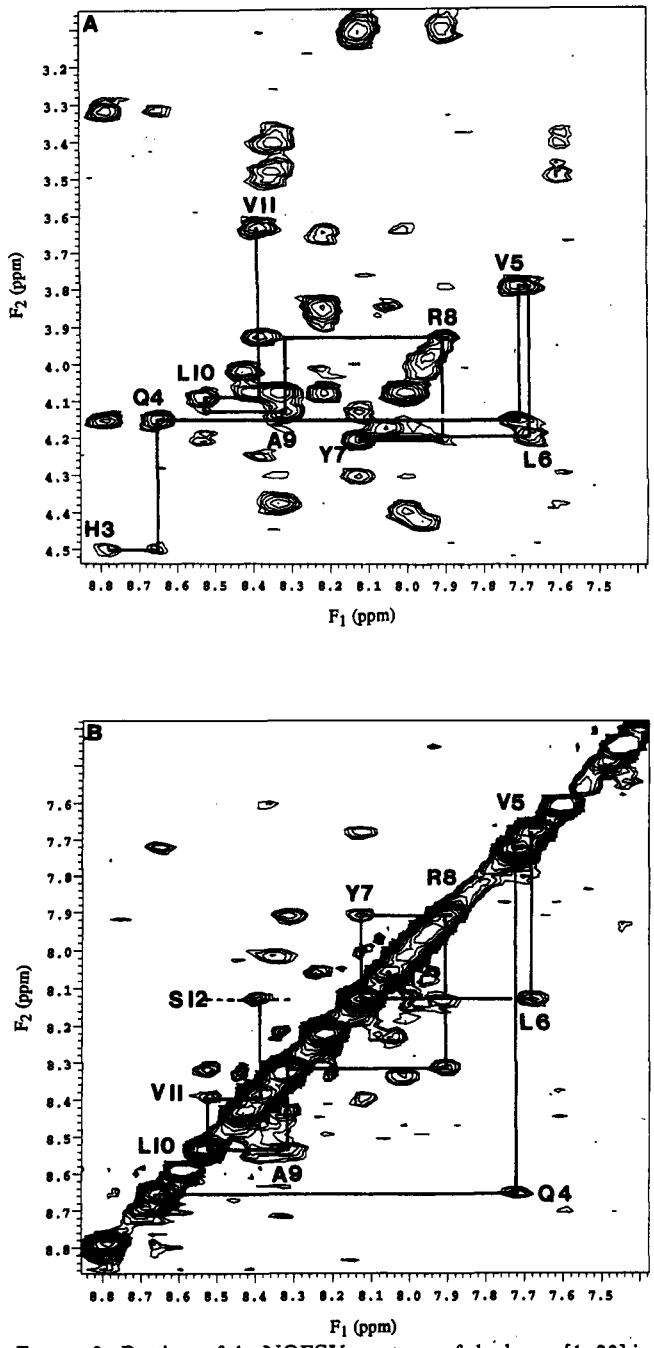

FIGURE 3: Portions of the NOESY spectrum of rhodanese[1–23] in 50% TFE: (A) NH-Hα region, with cross-peaks representing intraresidue correlations for H3-V11 labeled and (B) NH–NH region, with interresidue correlations for Q4–S12 labeled.

Solution Structure of Thiolase[1–21] Characterized by NMR. NMR spectra of thiolase[1–21] using <50% TFE contained very broad resonance lines, suggesting exchange broadening or aggregation. At 70% TFE, the resonances were much sharper. This solvent was suitable for two-dimensional NMR methods. Comparisons of CD spectra showed that the conformation of this peptide appeared to be similar in 70% TFE and SDS micelles, but was somewhat different in the presence of SUVs containing cardiolipin. On the basis of the intensity of the spectrum at 222 nm, the peptide was judged to retain significant α-helical content in the latter medium. To obtain a greater certainty in the conformational preferences of thiolase[1–21], both 70% TFE and PC micelles were chosen for the NMR studies.

Table 2: Chemical Shift Assignments for Rhodanese[1–23] in 50% TFE

residue	NH	Hα	Hβ	Hγ	others
Met1	NO[a]	4.26	2.23, 2.23	2.65, 2.60	
Val2	8.38	4.16	2.18	1.04, 1.00	
His3	8.79	4.51	3.36, 3.30		8.59; 7.30
Gln4	8.67	4.15	2.19, 2.19	2.57, 2.45	7.41, 6.78
Val5	7.74	3.80	2.20	1.08, 1.01	
Leu6	7.68	4.20	1.73	NA[b]	NA
Tyr7	8.13	4.21	3.10, 3.10		7.08; 6.80
Arg8	7.90	3.96	2.02, 2.02	1.91, 1.71	7.29; 3.23
Ala9	8.32	4.15	1.58		
Leu10	8.54	4.09	1.94, 1.59	1.81	0.90; 0.90
Val11	8.39	3.64	1.94	0.80, 0.80	
Ser12	8.14	4.31	4.13, 3.99		
Thr13	8.00	4.08	4.38	1.33	
Lys14	8.02	4.09	2.01, 2.01	1.54, 1.43	2.97, 2.97; 1.70, 1.70
Trp15	8.34	4.38	3.50, 3.40		9.67; 7.61; 7.45; 7.21 7.20; 7.10
Leu16	8.38	3.92	1.85, 1.85	1.76	0.96; 0.96
Ala17	8.43	4.03	1.53		
Glu18	8.32	4.09	2.18, 2.18	2.61, 2.49	
Ser19	8.21	4.09	3.87; 3.65		
Ile20	8.23	3.85	1.94	1.71, 1.16, 0.92	0.84
Arg21	8.06	4.19	1.96, 1.96	1.83, 1.72	7.24; 3.20
Ser22	7.98	4.43	4.06, 4.04		
Gly23	7.97	4.01, 3.49			7.46; 6.94

[a] Not observed. [b] Not assigned.

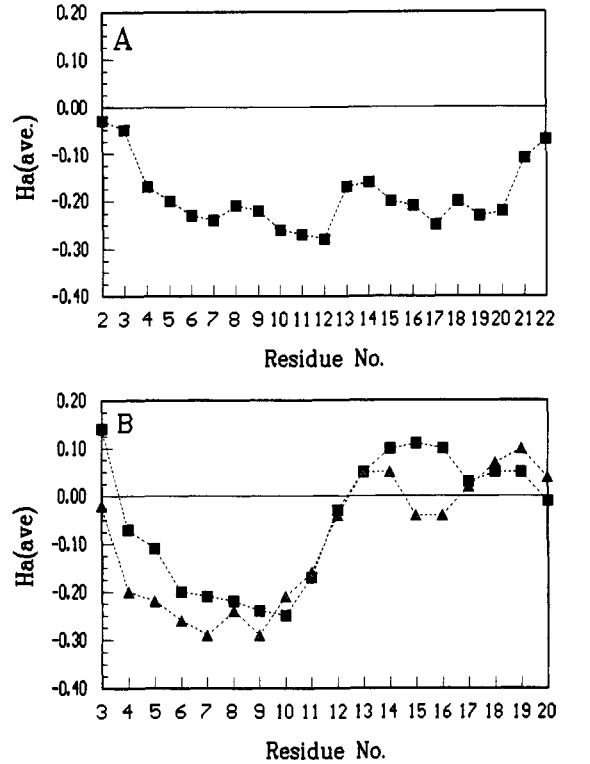

FIGURE 4: The relationship of α-proton chemical shift to random coil values for (A) rhodanese[1–23] in 50% TFE and (B) thiolase-[1–21] in 70% TFE and in solution with dodecylphosphatidylcholine micelles.

In 70% TFE, chemical shift assignments for each amino acid spin system were obtained from analyses of DQF-COSY and TOCSY spectra. All protons were identified without the use of NOESY spectra. Only the protons of the aromatic side chain of F8 were not identified. Discrimination between L3 and L4 was very difficult because of the chemical shift coincidence of the α-protons and many of the side-chain protons in 70% TFE. The resonances assigned to T16 were of very low intensity and were not observed in all spectra. Sequential residue assignments were made using the NOESY spectrum

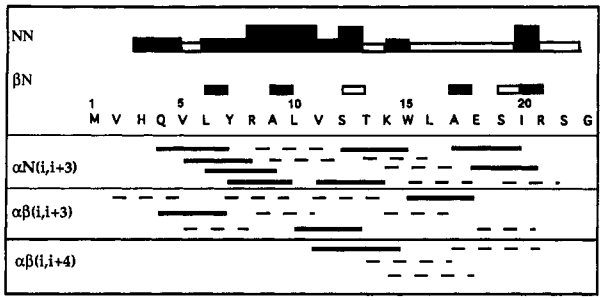

FIGURE 5: Inter-residue NOE tabulation for rhodanese[1–23] in 50% TFE. Open bars in the top part of the figure represent unresolved interactions. The height of these bars indicates the relative cross-peak intensity. Dashed lines in the lower part of the figure represent unresolved interactions.

and the known amino acid sequence (Figure 6). The chemical shift assignments are presented in Table 3.

As with rhodanese[1–23], secondary structure features were assessed by plotting the chemical shifts of α-protons relative to random coil values. The strong preference toward an upfield shift in residues 4–13 is indicative of an α-helix spanning these residues (Figure 4B). The dramatic change after K13 suggests that the helix comes to an end after their residue.

Analyses of inter-residue interactions in NOESY spectra indicate that thiolase[1–21] forms an α-helical structure between residues 4 and 14 in 70% TFE solution (Figure 7). Resolved $H\alpha_i$-HN_{i+3} interactions were observed for I9-A12 and V10-K13. Resolved $H\alpha_i$-$H\beta_{i+3}$ interactions were observed for L4-V7, V7-V10, F8-A11, I9-A12, V10-K13, and A11-R14. Medium-range interactions that could not be definitively assigned, due to spectral overlap, are noted in Figure 7. The observed interactions are characteristic of an α-helical conformation extending from L4 to R14.

In solution with PC micelles, thiolase[1–21] chemical shift assignments were made for main-chain and many side-chain protons using the TOCSY and DQF-COSY spectra. Several side-chain assignments as well as sequential assignments were made by comparing TOCSY and NOESY spectra. The entire M1 residue, the amide proton of A2, the δ-methyl group of I9 and one resonance in the F8 aryl group could not be assigned. The assignments are presented in Table 4.

Secondary structure was assessed by plotting α-proton chemical shifts relative to random-coil values. The results are similar to those obtained in 70% TFE solution, although the α-helix appears to begin at L3 rather than at L4. The results appear in Figure 4B.

Resolved $H\alpha_i$-HN_{i+3} interactions were observed for G6-I9, I9-A12, and V10-K13. Resolved $H\alpha_i$-$H\beta_{i+3}$ interactions were observed for L4-V7, R5-F8, G6-I9, V7-V10, F8-A11, I9-A12, and V10-K13. The interactions that have been observed are presented in Figure 8, and medium-range interactions that could not be definitively assigned, due to spectral overlap, are noted. The observed interactions are characteristic of an α-helical conformation extending from L4 to R14.

Interaction of Peptides with SUVs. A property that has been attributed to signal sequences is their ability to interact with lipid bilayers. Both rhodanese[1–23] and thiolase-[1–21] were shown to interact with phospholipid vesicles containing 30% cardiolipin/70% egg L-α-lecithin by measurements of steady-state fluorescence anisotropy. By this measure, neither peptide interacted with vesicles made from only L-α-lecithin. The anisotropy values for both peptides in buffer, 0% cardiolipin/100% lecithin, and 30% cardiolipin/70% lecithin are presented in Table 5. These results indicate the negatively charged head group is an important feature of

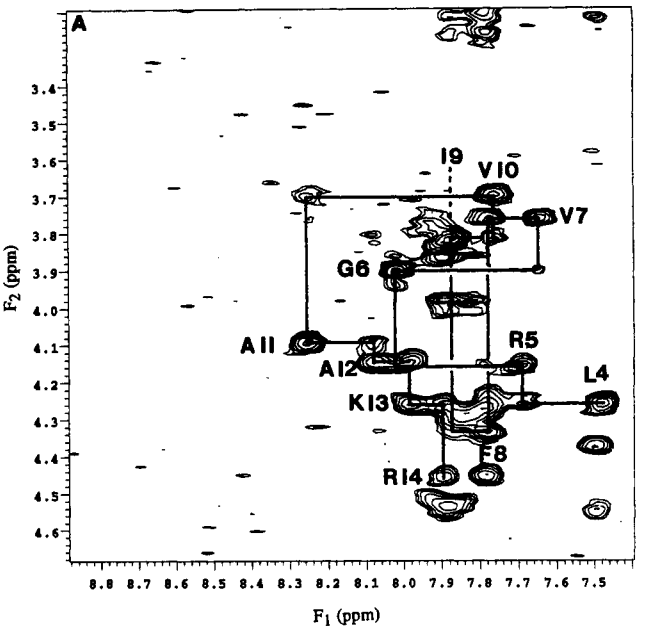

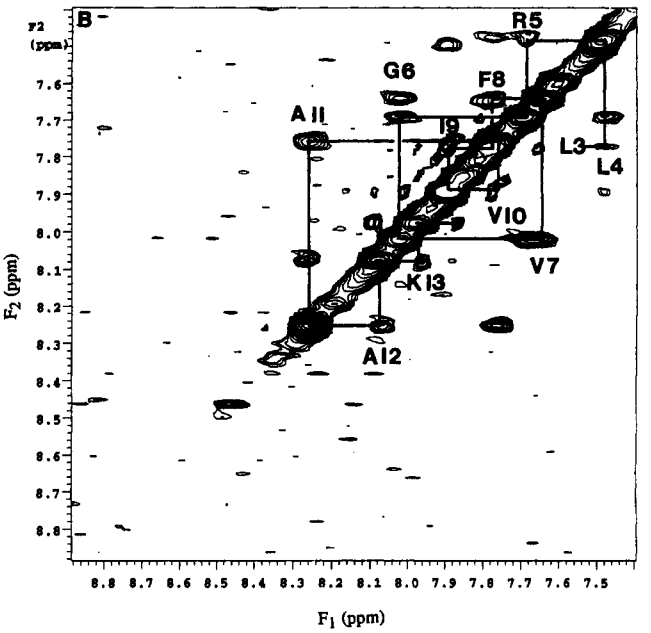

FIGURE 6: Portions of the NOESY spectrum of thiolase[1–21] in 70% TFE: (A) NH–Hα region, with cross-peaks representing intra-residue correlations for L4-R14 labeled and (B) NH–NH region, with interresidue correlations for L3-K13 labeled.

the interaction. The importance of the negatively charged head group in the interaction between signal peptides and liposomes has been demonstrated previously (Hoyt *et al.*, 1991; Zardeneta *et al.*, 1992; Wang & Weiner, 1994).

DISCUSSION

In these studies, three membrane model systems have been used to probe synthetic signal sequence structures in membrane mimetic surroundings. Trifluoroethanol has been used as a structure-promoting solvent in many NMR studies. Examples have been reported that demonstrate how peptides adopt their "native" structure when in TFE solution (Dyson *et al.*, 1988). However, the interaction of TFE with peptides can be expected to be rather symmetric, spatially, while there should be a

Table 3: Chemical Shift Assignments for Thiolase[1–21] in 70% TFE

residue	NH	Hα	Hβ	Hγ	others
Met1	NO[a]	NA[b]	NA	NA	
Ala2	7.78	4.74	1.28		
Leu3	7.78	4.27	1.66, 1.48	1.66	0.96; 0.92
Leu4	7.49	4.26	1.72, 1.67	1.67	0.98; 0.90
Arg5	7.69	4.16	1.94, 1.94	1.78, 1.76	7.18; 3.23
Gly6	8.02	3.89, 3.89			
Val7	7.63	3.76	2.14	1.00, 0.87	
Phe8	7.77	4.34	3.25, 3.21		7.25; NA; NA
Ile9	7.85	3.82	2.05	1.81, 1.25	0.99; 0.96
Val10	7.74	3.70	2.19	1.07, 0.97	
Ala11	8.23	4.10	1.47		
Ala12	8.05	4.14	1.43		
Lys13	7.96	4.25	1.98, 1.98	1.59, 1.55	3.00; 1.71
Arg14	7.89	4.46	2.02, 1.88	1.80, 1.69	7.11; 3.18
Thr15	7.70	4.48	4.11	1.20	
Pro16		4.37	2.21, 1.68	1.93, 1.87	3.80, 3.58
Phe17	7.48	4.54	3.23, 3.03		7.38; 7.31; 7.24
Gly18	7.88	4.00, 3.87			
Ala19	7.79	4.31	1.31		
Tyr20	7.84	4.54	3.15, 3.00		7.13; 6.84
Gly21	7.92	3.82, 3.82			6.91, 6.69

[a] Not observed. [b] Not assigned.

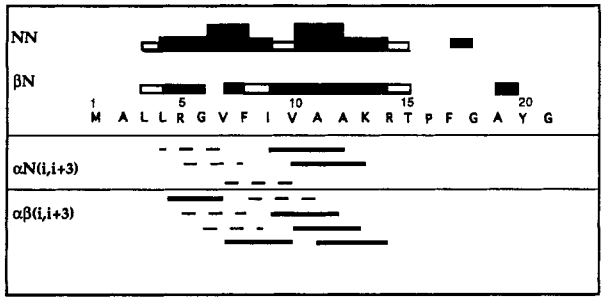

FIGURE 7: Inter-residue NOE tabulation for thiolase[1–21] in 70% TFE. Open bars in the top part of the figure represent unresolved interactions. The height of these bars indicates the relative cross-peak intensity. Dashed lines in the lower part of the figure represent unresolved interactions.

Table 4: Chemical Shift Assignments for Thiolase[1–21] with PC Micelles

residue	NH	Hα	Hβ	Hγ	others
Met1	NO[a]	NA[b]	NA	NA	
Ala2	NA	4.49	1.52		
Leu3	8.80	4.21	1.85, 1.67	1.68	1.07; 0.88
Leu4	8.42	4.12	1.83, 1.68	1.19	1.03; 0.93
Arg5	8.08	4.09	1.95, 1.95	1.76, 1.76	7.61; 3.32
Gly6	8.29	3.96, 3.96			
Val7	8.08	3.76	2.24	1.07, 0.88	
Phe8	8.10	4.31	3.32, 3.24		7.27; 7.19; NA
Ile9	8.10	3.85	2.08	1.76, 1.76, 1.02	NA
Val10	7.76	3.81	2.22	1.15; 1.030	
Ala11	8.41	4.11	1.45		
Ala12	8.23	4.10	1.42		
Lys13	7.82	4.28	2.02, 1.58	1.76, 1.68	3.00; 1.68
Arg14	7.95	4.50	2.09, 1.89	1.75, 1.75	7.64; 3.24
Thr15	7.88	4.26	4.26	1.34	
Pro16		4.11	1.95, 1.46	1.73, 1.73	3.86, 3.53
Phe17	8.00	4.62	3.33, 3.04		7.28; 7.21; 7.14
Gly18	8.37	4.00, 3.94			
Ala19	8.16	4.31	1.35		
Tyr20	8.12	4.51	3.17, 3.03		7.03; 6.74
Gly21	8.28	3.88, 3.88			6.81, 6.59

[a] Not observed. [b] Not assigned.

sidedness to the peptide–membrane interaction. Micelles are another form of membrane-mimetic medium which have been shown to be adequate models for membranes in NMR studies (Brown, 1979; Gierasch *et al.*, 1982). Micelles discriminate

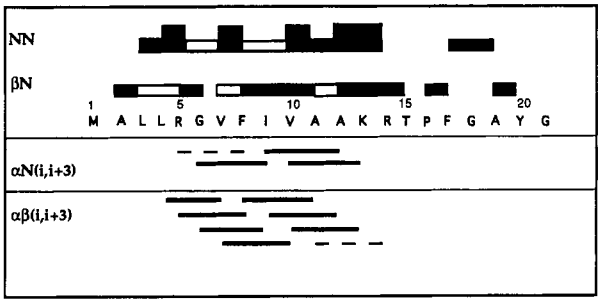

FIGURE 8: Inter-residue NOE tabulation for thiolase[1–21] in solution with dodecylphosphatidylcholine micelles. Open bars in the top part of the figure represent unresolved interactions. The height of these bars indicates the relative cross-peak intensity. Dashed lines in the lower part of the figure represent unresolved interactions.

Table 5: Fluorescence Anisotropy Values for Rhodanese[1–23] and Thiolase[1–21] at 25.5 °C

	r^a	n^b	σ
Rhodanese[1–23]			
phosphate buffer	0.040	2	0.007[c]
0% CL SUVs	0.045	5	0.007[d]
30% cardiolipin SUVs	0.104	5	0.0005[d]
Thiolase[1–21]			
phosphate buffer	0.026	2	0.001[c]
0% cardiolipin SUVs	0.031	2	0.007[c]
30% cardiolipin SUVs	0.138	4	0.006[d]

[a] Anisotropy (mean value). [b] Number of measurements. [c] Average deviation. [d] Standard deviation.

polar from apolar components. However, they lack the bilayer of a membrane and, with a small surface area, their correspondence to the biological condition is not complete. Liposomes (SUVs) are composed of lipid bilayers and have the size necessary to mimic the biologically relevant interaction. Because they are smaller than organelles, one must consider that lipid packing may be different, especially because of the curvature of the SUVs (Gennis, 1989). Each of these model systems represents the biological condition to some extent, although not completely. Therefore, it may be premature to draw conclusions on the most likely polypeptide conformation on the basis of data obtained in only one medium. It is important to look for conformational conformity across several model systems for assurance that the results really correspond to the conditions represented by the models.

Information obtained from CD spectra in all three membrane mimetic environments shows that rhodanese[1–23] forms an α-helical structure for virtually the entire length of the polypeptide. For this reason, the structure obtained from NMR spectra in 50% TFE cannot differ significantly from that involved in interactions with liposomes. The present results suggest that this peptide has a strong preference for the α-helical conformation in lipid-like environments. In the crystal structure of the mature bovine protein (minus M1), the α-helix begins at residue 11. In this case, the N-terminus is not in a lipid environment, so the structure must be viewed in the context of the protein crystal and not that of the membrane.

In contrast, the CD spectra of thiolase[1–21] appear to arise from conformations that differ depending upon the lipid-like medium. The value of ca. 52% α-helix estimated from the molar ellipticity at 222 nm is in good agreement with the NMR data, in which the helix spans residues 4–14. The amount of α-helix estimated by spectral deconvolution varies between 25% and 45%. The shape of the spectra are consistent with an increase in the amount of β-structure in the progression

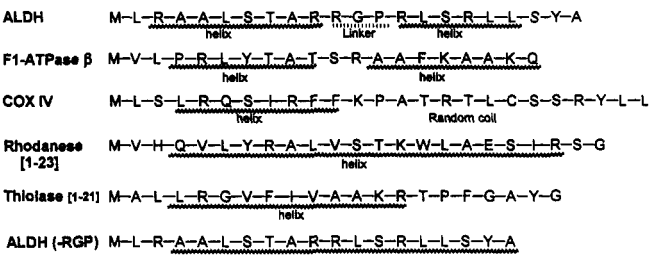

FIGURE 9: Signal sequences whose structures have been determined using 2D-NMR techniques. The medium is indicated for each peptide. ALDH–micellar (Karslake, et al., 1990); COX IV–micellar (Endo, et al., 1989); rhodanese–50% TFE (this study); thiolase–70% TFE and micellar (this study); F_1-ATPase β–50% TFE (Bruch & Hoyt, 1992). For the latter, the C-terminal helix was observed more readily at 5 °C than under ambient conditions. For ALDH, the three C-terminal residues come after the processing site. The tyrosine at position 20 in the peptide replaces alanine, which is found at this position on the protein.

from solvent, TFE, to micelles to SUVs. The sequential NH–NH interactions observed among F17, G18, and A19 (Figures 7 and 8) are incompatible with the presence of β-structure in this region of the peptide. Otherwise, no evidence for β-structure could be found in the NOESY spectra obtained in 70% TFE or with micelles.

Steady-state fluorescence anisotropies were measured in the absence and presence of liposomes to investigate whether the peptides associate with liposomes. The data in Table 5 demonstrate that an interaction occurs between the synthetic signal sequences and liposomes and that this interaction requires the presence of cardiolipin. Anisotropy values are consistent with those previously reported for tryptophan in oligopeptide–liposome interactions (Jain *et al.*, 1985). The value of 0.1 for rhodanese[1–23] suggests that the tryptophan side chain may be immobilized when the peptide binds to the liposome. The α-helical structure of rhodanese[1–23] places the tryptophan on the hydrophilic side of the amphiphilic α-helix, so that if the peptide is bound to the liposome with the hydrophobic face buried in the bilayer (Thornton *et al.*, 1993), the tryptophan side chain may retain some mobility. This orientation for tryptophan is reasonable, since neutron diffraction studies (Jacobs & White, 1989) have shown that tryptophan side chains can be found predominantly near the lipid head groups when interacting with liposomes. The anisotropy near 0.15 for thiolase[1–21] is consistent with the interpretation that the tyrosine side chain is immobilized in the liposome. Since we do not know with certainty the structure of the C-terminal end of the signal sequence when it is bound to the liposome, we cannot speculate how the tyrosine interacts.

It was the intent of this research to learn whether the N-terminal sequences for proteins that are not processed have some structural characteristic that distingushes them from cases where the signal sequence is cleaved. Thus far, the structures of five mitochondrial signal sequences have been determined. They are shown in Figure 9. The greater length of the N-terminal α-helix is evident for the peptides that correspond to nonprocessed signal sequences. Thus, a pattern appears to be emerging. Signal sequences which tend to form continuous helices of more than 11 residues are not processed, while those that tend to form shorter, or noncontinuous, helices are processed.

In addition to the work from our laboratories, in which the RGP deletion altered ALDH so that it was imported without signal sequence processing, there is other evidence which shows that amino acid deletions can lead to the elimination of processing. Deletion of residues 2–5 in the COX-IV signal

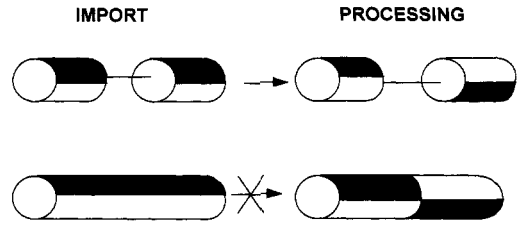

FIGURE 10: Structural model depicting possible conformational requirements of mitochondrial signal sequences. The top drawing represents a sequence, with conformational flexibility, that can adopt the conformations necessary for both import and processing. The bottom drawing reperesents a long helical conformation which can adopt only the conformation required for the import function.

sequence produced a precursor protein that was imported but not processed (Hurt *et al.*, 1986). If it is assumed that the conformational preferences of the deletion mutant are the same as for the native sequence, this result would be contrary to the model presented here, involving the long, continuous helix. The structural consequences of amino acid deletions are known only for the ALDH case, in which the structure containing two helices becomes one longer helix after deletion. It will be necessary to study the structure of the COX IV deletion mutant to more completely understand how this mutation effects processing.

It has been demonstrated that a native sequence that can form a stable amphiphilic α-helix at the pre-protein N-terminus is an essential requirement for successful import (Roise *et al.*, 1988; Wang & Weiner, 1993). While amphiphilicity may be a crucial structural component for interaction with the import machinery, other structural features may be important for the proteolytic step (Figure 10). The flexible region of signal sequences may be the source of their multifunctional character. One structure could allow for the attachment of the precursor protein to the mitochondrial membrane or import receptors, while a different conformation could be necessary for recognition by the protease. In the case of signal sequences that have α-helices extending beyond 11 residues, or three turns, the necessary flexibility may not be present to adopt the conformation recognized by the protease. Alternatvely, the longer helices may have greater affinity for the inner mitochondrial membrane. The imported protein would become attached to the membrane, making it impossible for the protease to cleave the signal sequence. In either case, it would be the length and stability of the α-helix which interferes with proteolytic processing.

ACKNOWLEDGMENT

The authors wish to thank Profs. R. A. Dilley for the use of the fluorescence spectrophotometer and W. A. Cramer for the use of the polarizers employed in the anisotropy measurements.

REFERENCES

Allison, D. S., & Schatz, G. (1986) *Proc. Natl. Acad. Sci. U.S.A.*, *83*, 9011–9015.

Arakawa, H., Takiguchi, M., Amaya, Y., Nagata, S., Hayashi, H., & Mori, M (1987) *EMBO J. 6*, 1361–1366.

Arakawa, H., Amaya, Y., & Mori, M (1990) *J. Biochem. 107*, 160–164.

Arretz, M., Schneider, H., Guiard, B., Brunner, M., & Neupert, W. (1994) *J. Biol. Chem. 269*, 4959–4967.

Bax, A., & Davis, D. G. (1985) *J. Magn. Reson. 65*, 355–360.

Braunschweiler, L., & Ernst, R. R. (1983) *J. Magn. Reson. 53*,

521–528.
Brown, L. R. (1979) *Biochim. Biophys. Acta 557*, 135–148.
Bruch, M. D., & Hoyt, D. W. (1992) *Biochim. Biophys. Acta 1159*, 81–93.
Endo, T., Shimada, I., Roise, D., & Inagaki, F. (1989) *J. Biochem. 106*, 396–400.
Gavel, Y. & von Heijne, G. (1990) *Protein Eng. 4*, 33–37.
Géli, V. (1993) *Proc. Natl. Acad. Sci. U.S.A. 90*, 6247–6251.
Gierasch, L. M., Lacy, J. E., Thompson, K. F., Rockwell, A. L., & Watnick, P. (1982) *Biophys. J. 37*, 275–284.
Glaser, S. M., & Cumsky, M. G. (1990) *J. Biol. Chem. 265*, 8808–8816.
Hannavy, K., Rospert, S., & Schatz, G. (1993) *Curr. Opinion Cell Biol. 5*, 694–700.
Hartl, F.-U., Pfanner, N., Nicholson, D. W., & Neupert, W. (1989) *Biochim. Biophys. Acta 988*, 1–45.
Horwich, A. L., Kalousek, F., Fenton, W. A., Pollock, R. A., & Rosenberg, L. E. (1987) *J. Cell. Biol. 105*, 669–677.
Horwich, A. L., Cheng, M., West, A., & Pollock, R. A. (1991) *Curr. Top. Microbiol. Immunol. 170*, 1–42.
Hoyt, D. W., Cyr, D. M., Gierasch, L. M., & Douglas, M. G. (1991) *J. Biol. Chem. 266*, 21693–21699.
Huang, C. (1969) *Biochemistry 8*, 344–352.
Jacobs, R. E., & White, S. H. (1989) *Biochemistry 28*, 3421–3437.
Jain, M. K., Rogers, J., Simpson, L., & Gierasch, L. (1985) *Biochim. Biophys. Acta 816*, 153–162.
Jeng, J., & Weiner, H. (1991) *Arch. Biochem. Biophys. 289*, 214–222.
Karslake, C., Piotto, M., Pak, Y. K., Weiner, H., & Gorenstein, D. G. (1990) *Biochemistry 29*, 9872–9878.
Lakowicz, J. R. (1983) *Principles of Fluorescence Spectroscopy*, pp 112–150, Plenum Press, New York, NY.
Marion, D., & Wüthrich, K. (1983) *Biochem. Biophys. Res. Commun.* 4113, 967–974.
Pak, Y. K., & Weiner, H. (1990) *J. Biol. Chem. 265*, 14298–14307.
Piantini, U., Sorensen, O. W., & Ernst, R. R. (1982) *J. Am. Chem. Soc. 104*, 6800–6801.
Ploegman, J. H., Drent, G., Kalk, K. H., Hol, W. G. J., Heinrikson, R. L., Keim, P., Weng, L., & Russell, J. (1978) *Nature 273*, 124–129.
Rance, M., Sorensen, O. W., Bodenhausen, G., Wagner, G., Ernst, R. R., & Wüthrich, K. (1983) *Biochem. Biophys. Res. Commun. 117*, 479–485.
Roise, D., Theiler, F., Horvath, S. J., Tomich, J. M., Richards, J. H., Allison, D. S., & Schatz, G. (1988) *EMBO J. 7*, 649–653.
Shoemaker, K. R., Kim, P. S., York, E. J., Stewart, J. M., & Baldwin, R. L. (1987) *Nature 326*, 563–567.
States, D. J., Haberkorn, R. A., & Rueben, D. J. (1982) *J. Magn. Reson. 48*, 286–292.
Thornton, K., Wang, Y., Weiner, H., & Gorenstein, D. (1993) *J. Biol. Chem. 268*, 19906–19914.
Vassarotti, A., Stroud, R., & Douglas, M. (1987) *EMBO J. 6*, 705–711.
Wang, Y., & Weiner, H. (1994) *Biochemistry* (submitted for publication).
Wishart, D. S., Sykes, B. D., & Richards, F. M. (1992) *J. Mol. Biol. 222*, 311–333.
Zardeneta, G., & Horowitz, P. M. (1992) *J. Biol. Chem. 267*, 24193–24198.